Metrol. Meas. Syst., Vol. 28 (2021) No. 4, pp. 803–812
DOI: 10.24425/mms.2021.138578

PAN POLSKA AKADEMIA NAUK

METROLOGY AND MEASUREMENT SYSTEMS
Index 330930, ISSN 0860-8229
www.metrology.wat.edu.pl

M&MS

IMPROVING THE ACCURACY OF THE NDIR-BASED CO_2 SENSOR FOR BREATH ANALYSIS

Artur Prokopiuk, Zbigniew Bielecki, Jacek Wojtas

Military University of Technology, Institute of Optoelectronics, 00-908 Warsaw, 2 Gen. Sylwestra Kaliskiego St.
(✉ *artur.prokopiuk@wat.edu.pl*, +48 261 83 77 40, *zbigniew.bielecki@wat.edu.pl*, *jacek.wojtas@wat.edu.pl*)

Abstract

The paper presents an analysis and practical study of the temperature and pressure influence on a non-dispersive infrared (NDIR) sensor for measuring the concentration of carbon dioxide in human breath. This sensor is used for monitoring patients' carbon dioxide (CO_2) in the exhaled air. High precision and accuracy of CO_2 concentration measurements are essential in air sampling systems for breath analysers. They, however, require an analysis of the influence of the human exhaled air pressure and temperature on the NDIR CO_2 sensor. Therefore, analyses of the changes in concentration were carried out at a pressure from 986 mbar to 1027 mbar and a temperature from 20°C to 36°C. Finally, corresponding correction coefficients were determined which allow to reduce the relative uncertainty of CO_2 sensor measurements results from 19% to below 5%.

Keywords: NDIR, CO_2 sensors, breath analysis, absorption spectroscopy.

1. Introduction

Analysis of chemical composition of the human exhaled air is one of the novel non-invasive techniques in medical screening [1, 2]. So far more than 3000 different gaseous components have been found [3], and many of them are biomarkers with concentration (at the *ppb – ppm* level) corresponding to a specific disease. During exhalation, the biomarkers concentrations change depending on specific parts of the human exhalation, the so-called phases. The air from the gas exchange in the alveoli (phase III), containing the products of the body metabolic processes, is the primary source of medical data. One of the methods of this phase of selecting the part of the exhaled air is based on the analysis of changes in the concentration of *carbon dioxide* (CO_2). However, a high level of water vapor and changes in the exhaled air pressure and temperature may lead to erroneous measurements. Therefore, it is necessary to minimize these adverse effects to ensure the high precision of air sampling devices for the biomarkers analysis.

Changes in CO_2 concentration during exhalation can be shown in a capnography waveform, also called a capnogram [4]. The analysis of the waveform allows dividing the exhalation into

Article history: received June 20, 2021; revised August 16, 2021; accepted August 27, 2021; available online September 2, 2021.

four phases. The analyzed air in phase I is usually free of CO_2 and endogenous volatile organic compounds. In phase II, there is a rapid increase in the carbon dioxide concentration due to an increasing proportion air from the alveolar fraction. During this phase, the contents of the alveoli are emptied. Phase III, also known as the "expiratory plateau", then begins with the maximum CO_2 concentration. The $PetCO_2$ point (partial pressure of the end-tidal CO_2) defines the end-expiratory phase (Table 1).

Table 1. Exhalation phases determined using exhaled CO_2 concentration [5].

Exhalation phase	**Characteristics**	**Capnogram**
I	Beginning of exhalation. Air from the upper respiratory tract not involved in gas exchange with blood	Low CO_2 concentration (close to the atmospheric one)
II	Mixture of air from dead volume and alveolar air	Rapid increase of CO_2 concentration (up to about 3%÷5%)
III	Air from alveoli	Slow increase of CO_2 concentration until it reaches its maximum value ($PetCO_2$)
IV	End of exhalation and beginning of the next inhalation process	Rapid decrease in CO_2 concentration to atmospheric air concentration levels

2. Research tasks and methods

2.1. Sensor analytical model

The purpose of analyzing the sensor performance in the absence of CO_2 is to determine the maximum power incident on the detector as well as the ratio of the signal power to the noise power. Various sensors can be used to measure the carbon dioxide concentration, however, *non-dispersive infrared* (NDIR) type sensors are most commonly used in capnography [6–8] because of their selectivity, sensitivity, and rapid measurements [9]. The gas pressure and temperature changes can make a difference in the number of gas molecules and in the shape of absorption lines. The exhaled air is a compressible gas whose state is described by the equation:

$$PV = znRT, \tag{1}$$

where: P – gas pressure, V – –gas volume, z- compressibility factor, n – number of gas moles, R – universal gas constant ($R = 8.314$ J/mol·K), T – gas temperature. Thus, the concentration of CO_2 in the exhaled air is directly proportional to the pressure and inversely proportional to the temperature of the air sample. This results in erroneous results of concentration measurements. Therefore, a theoretical NDIR type CO_2 sensor model was developed to evaluate these errors.

The model idea is shown in Fig. 1. The sensor consists of a radiation source (RS), a detector (DET), and an optical filter (F). A gas sample (G) is analyzed in a gas cell (GC) of length L where absorption of the radiation takes place at a specific range of wavelengths emitted from the RS, resulting in a change of the output signal (SIG).

Detection is based on a comparison of two detector signals corresponding to the receiving optical powers for the empty $P_0(\lambda)$ and air-filled $P_{ABS}(\lambda)$ gas cell. The power of the radiation incident on the detector surface after passing through the gas can be determined from the Lambert–Beer law [10]:

$$P_{ABS}(\lambda) = P_0(\lambda)\, \mathrm{e}^{-\alpha(\lambda)L}, \tag{2}$$

Metrol. Meas. Syst., Vol. 28 (2021), No. 4, pp. 803–812
DOI: 10.24425/mms.2021.138578

where: $\alpha(\lambda)$ – gas absorption coefficient determined as $\alpha = \sigma \cdot C$ (σ is the gas absorption cross section and C – gas concentration).

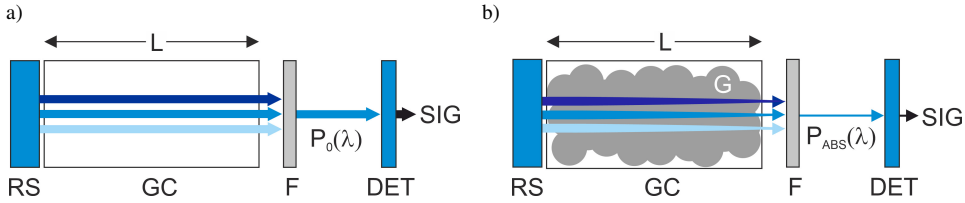

Fig. 1. Components of the NDIR sensor: $P_0(\lambda)$ is the radiation power incident on the detector with absence of gas in the gas cell (a), $P_{ABS}(\lambda)$ is the radiation power incident on the detector when the test gas is present in the gas cell (b).

Parameters of the NDIR sensor model components for determination of spectral characteristics of radiation absorption are shown in Table 2.

Table 2. Main parameters of the NDIR sensor model components.

Component	Parameters	References
Radiation source	Centre wavelength $\lambda = 4.3$ µm Radiation power $P \geq 0.3$ mW Beam divergence $\leq 50°$	[11]
Gas cell	Cell length $L = 2$ cm Transmission range $\geq 4.1 \div 4.3$ µm	[12]
Optical filter	Centre wavelength $\lambda = 4.2$ µm $FWHM \leq 120$ nm	[13]
Radiation detector	Sensitivity range $\geq 4.1 \div 4.3$ µm Normalized detectivity $D^* \geq 8 \cdot 10^{10}$ cm·Hz$^{1/2}$/W Current responsivity $R_i \geq 1.3$ A/W Active area $A \geq 1 \times 1$ mm^2 Time constant $\tau \leq 80$ ns	[14]

Analysis of the absorption spectra was performed using the Hitran-PC software version 4.1 and the program database version 2008. Figure 2 presents the simulated results of spectral characteristics of the transmitted LED radiation in a gas cell in two cases: empty (before absorption) and filled with the exhaled air. Analytical calculations enabled identification of basic phenomena occurring in the NDIR sensor. The following assumptions were made in the calculations and subsequent analyses: the analyzed gas is homogeneous inside the gas cell, there are no geometrical losses in the gas cell, no other gases, and apart from absorption, there are no other phenomena occurring in the tested gas (scattering, refraction).

The basis of physical phenomena in the sensor was analyzed in the absence of the analyzed gas in the gas cell ($\alpha = 0$) and in the presence of a 0.5% CO_2 concentration ($\alpha > 0$) inside the gas cell. For different pressures and temperatures, human exhaled air absorbance and *signal-to-noise ratio* (SNR) were calculated to estimate the influence of these parameters on accuracy of the NDIR sensor.

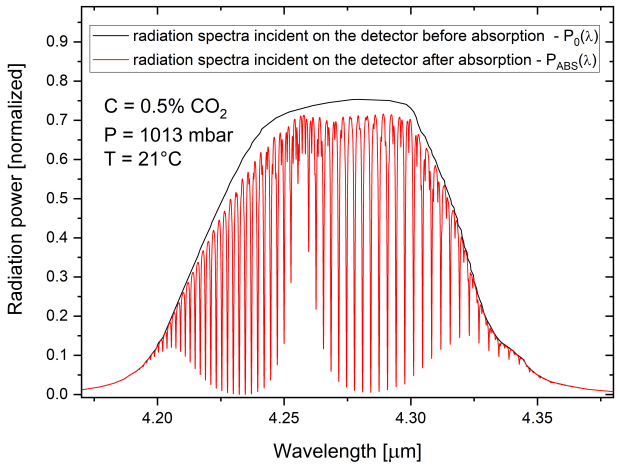

Fig. 2. Spectrum of LED radiation after passing through the empty (black line) and the breath-filled gas cell (red line).

2.2. Analysis of the influence of pressure and temperature

The detector noise level was calculated. The RMS value of thermal noise current I_{nt} was determined using the equation [15]:

$$I_{nt} = \frac{R_i(\lambda)\sqrt{\Delta f \cdot A}}{D^*}, \tag{3}$$

where $R_i(\lambda)$ is the spectral current responsivity and Δf is the detector noise bandwidth. The *noise equivalent power* (NEP) was calculated from the formula:

$$NEP = \frac{I_{nt}}{R_i(\lambda)}. \tag{4}$$

For noise bandwidth $\Delta f = 3.14$ MHz the values of these parameters are $I_{nt} = 2.9$ nA and NEP = 2.2 nW, respectively. Including LED radiation divergence, optical filter transmission, detector area and length of the gas cell, radiation power incident on the detector will be $P_0 = 18.0$ nW which generates a photocurrent I_f of 22.5 nA. The photocurrent will generate shot noise I_{ns} which can be estimated using the formula:

$$I_{ns} = \sqrt{2e \cdot I_f \cdot \Delta f}. \tag{5}$$

The estimated value of shot noise $I_{ns} = 0.15$ nA. The signal-to-noise ratio can be expressed by the formula:

$$SNR = 20 \log \frac{I_f}{\sqrt{I_{ns}^2 + I_{nt}^2}}. \tag{6}$$

The determined *SNR* is ≈ 17.85 dB.

When a CO_2 sample is present in the gas cell, some of the radiation will be absorbed by the gas. Based on the characteristics shown in Fig. 2, P_{ABS} will decrease to 17.2 nW. This means that there was a 4.4% decrease in the optical signal power due to absorption.

Metrol. Meas. Syst., Vol. 28 (2021), No. 4, pp. 803–812
DOI: 10.24425/mms.2021.138578

Assuming air pressure conditions from 955 mbar to 1074 mbar and the fact that the pressure of the exhaled air should be 20 mbar higher than the atmospheric one [16], the analysis of the pressure influence in the range from 955 mbar to 1074 mbar was taken into account. Reducing the gas pressure, reduces its maximum value (Fig. 3a). The change in the air pressure from the minimum of the assumed range to the maximum causes an increase in the mean absorbance to the level of 12.5% (Fig. 3b). Consequently, it reduces the radiation power incident on the detector and reduces the output SNR from 9.77 to 9.72.

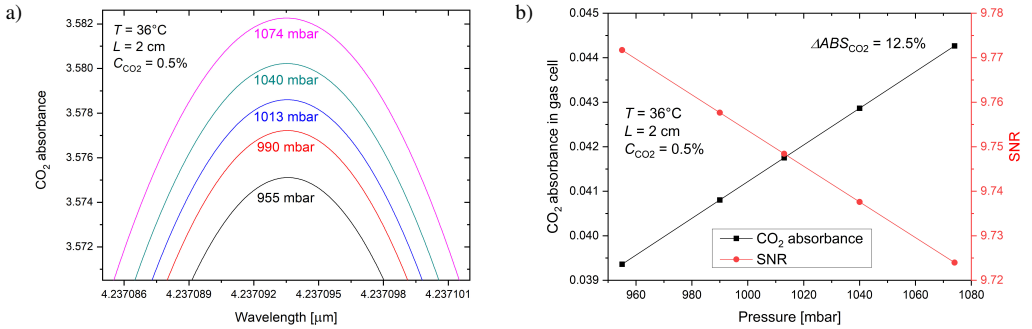

Fig. 3. CO_2 absorbance changes on the selected gas absorption line (a), CO_2 absorbance in the gas cell and SNR as a function of human exhaled air pressure (b).

Next, the influence of gas temperature changes from room temperature (about 20°C) to the maximum temperature of the exhaled air (about 36°C) [17] on the NDIR sensor output signal was analysed. A decrease in gas temperature causes a decrease in the maximum absorbance value (Fig. 4a). However, an increase in gas temperature causes a decrease in gas absorbance to the level of 5.3% (Fig. 4b). Increasing gas temperature inside the gas cell increases the power of radiation incident on the detector leading to an increase in SNR from 9.72 to 9.75.

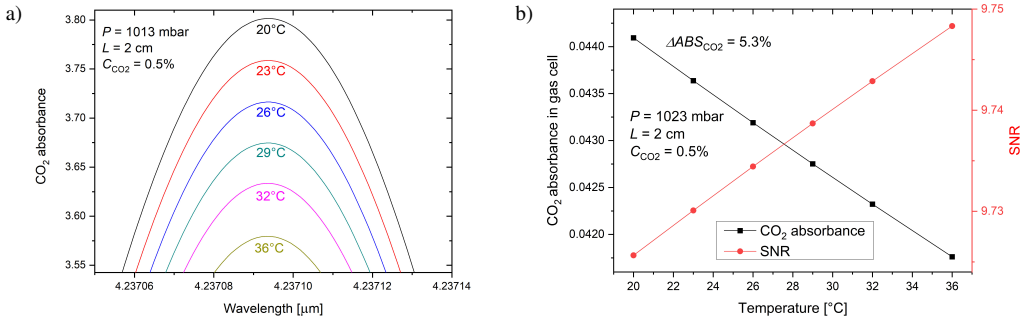

Fig. 4. CO_2 absorbance changes on the selected gas absorption line (a), CO_2 absorbance in the gas cell and SNR as a function of human exhaled air temperature (b).

As observed, the changes in gas temperature and pressure affect only the changes in gas absorbance, without significantly (about 0.3% ÷ 0.5%) affecting the SNR ratio. To summarize, increasing the accuracy of CO_2 concentration measurements with the NDIR sensor can be obtained by applying correction factors depending on the temperature and pressure of the tested gas sample.

3. Experiment

Theoretical analysis of the sensor model was experimentally verified using a UTECH UT100C ETCO2 sensor [18]. An MKS Type 1179A mass flow controller (MFC) was supplied with gas from a cylinder with dry synthetic air of a 5% CO_2 concentration. Tests were carried out from atmospheric pressure (986 mbar) to the pressure of 1027 mbar for the CO_2 sensor test below and above a standard pressure of 1013.25 mbar. Temperature was regulated using a UF30 Memmert universal oven model [19]. A BMP280 pressure and temperature sensor (absolute pressure accuracy of 1.0 mbar, absolute temperature accuracy of 0.5°C) was placed in the NDIR CO_2 sensor air stream, Fig. 5.

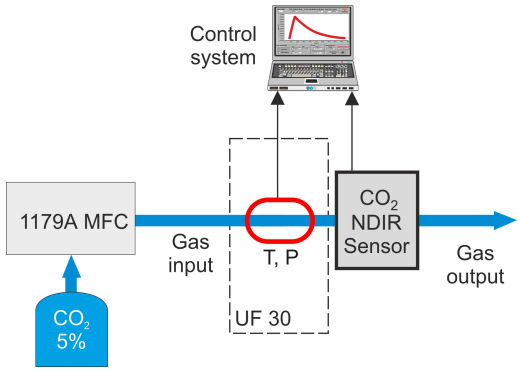

Fig. 5. Experimental setup for testing the CO_2 sensor. T – temperature sensor, P – pressure sensor.

Preliminary tests show that the humidity of the air sample did not affect the $\delta = 5\%$ uncertainty of the CO_2 sensor. Dependence of the NDIR sensor readouts when the pressure changes from 986 mbar to 1027 mbar is shown in Fig. 6.

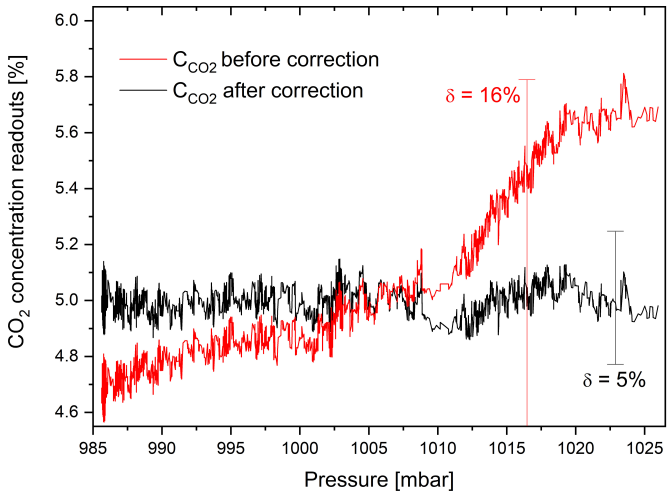

Fig. 6. Pressure influence on the UT100C CO_2 sensor readouts before and after correction.

Metrol. Meas. Syst., Vol. 28 (2021), No. 4, pp. 803–812
DOI: 10.24425/mms.2021.138578

The experiments confirmed that the CO_2 sensor measurements depend on the pressure of the flowing air. For low pressures, the sensor readouts were decreased while for higher pressures, sensor readouts were increased. Therefore, it was necessary to correct the sensor indications. The pressure (P) influence correction function was evaluated by an experimental approximation determined with the linear fit ($R^2 = 0.906$) by the OriginPro 2020 software and described by the formula:

$$C_{CO2} = C_{SCO2} \frac{208.2466}{P - 792.5177}, \tag{7}$$

where: C_{CO2} – CO_2 concentration after correction [%], C_{SCO2} – CO_2 concentration before correction [%].

An analogous procedure was carried out to study the effect of temperature on CO_2 sensor readouts. The BMP280 sensor was used to measure the temperature. The results are shown in Fig. 7.

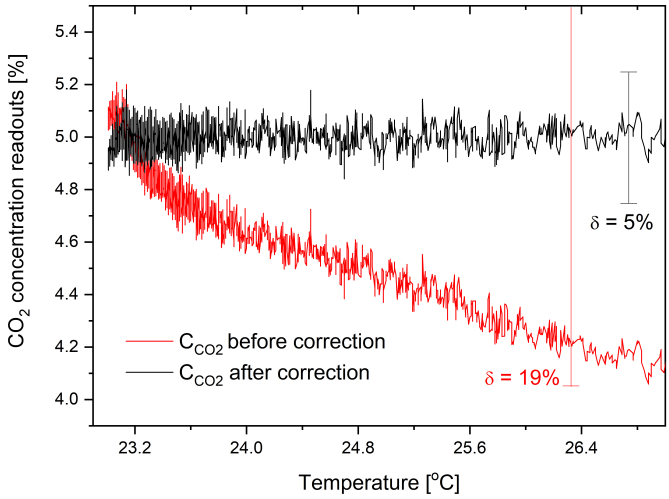

Fig. 7. Temperature influence on UT100C CO_2 sensor readouts before and after correction.

As the temperature increased, the CO_2 concentration measured with the NDIR sensor decreased at a rate of approximately 0.05%/°C. Therefore, the temperature (T) influence correction function was evaluated by the experimental approximation method determined with the linear fit ($R^2 = 0.883$) by the OriginPro 2020 software as:

$$C_{CO2} = C_{SCO2} \left(0.0102 \cdot T + 0.76212\right), \tag{8}$$

where: C_{CO2} – CO_2 concentration after correction [%], C_{SCO2} – CO_2 concentration before correction [%].

Based on the proposed CO_2 sensor readout correction functions (7) and (8), correction factors were determined to minimize the impact of temperature and pressure on the UT100C carbon dioxide NDIR sensor readouts (Fig. 8). In this way, the relative uncertainty of the sensor measurements was reduced from $\delta = 19\%$ to $\delta = 5\%$.

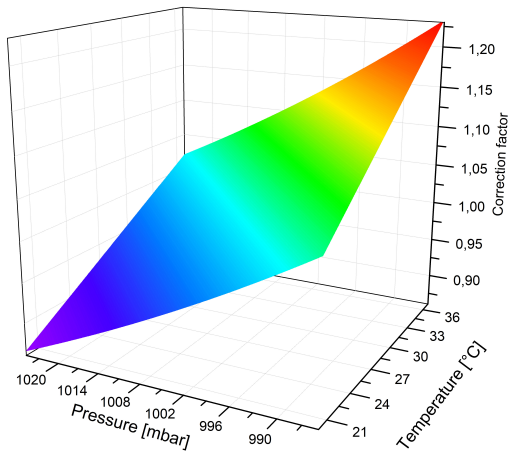

Fig. 8. Correction factors for pressure and temperature influence on CO_2 sensor measurements.

4. Conclusions

NDIR CO_2 sensors are commonly used for analysing the concentration of carbon dioxide exhaled by patients. However, the pressure and temperature of the air flowing through the sensor typically are not measured during breath, which leads to erroneous measurements. Since there is a need to accurately measure CO_2 concentration in devices for collecting and extracting specific phases from exhaled air samples, a correction of these measurements had to be performed for the sensor of the NDIR type. The influence of pressure and temperature was demonstrated both theoretically and experimentally and correction factors for these phenomena were developed to reduce the relative uncertainty of the measurements for the UT100C type CO_2 sensor from 19% to below 5%. Due to analogous phenomena occurring in other NDIR sensors, conducting a similar analysis should be taken into account.

Acknowledgements

The results of the research carried out in the laboratory of the Institute of Optoelectronics of the Military University of Technology have been published with the financial support of the project entitled "Development of structure technology for single-mode cascade lasers for applications in optical gas detection systems" (ID: 347510) no. TECHMATSTRATEG1/ 347510/15/NCBR/2018.

References

[1] Chludziński, T., & Kwiatkowski, A. (2020). Exhaled breath analysis by resistive gas sensors. *Metrology and Measurement Systems*, *27*(1), 81–89. http://dx.doi.org/10.24425/mms.2020.131718

[2] Bielecki, Z., Stacewicz, T., Wojtas, J., Mikołajczyk, J., Szabra, D., & Prokopiuk, A. (2018). Selected optoelectronic sensors in medical applications. *Opto-Electronics Review*, *26*(2), 122–133. https://doi.org/10.1016/j.opelre.2018.02.007

[3] Buszewski, B., Kęsy, M., Ligor, T., & Amann, A. (2007). Human exhaled air analytics: biomarkers of diseases. *Biomedical Chromatography*, *21*(6), 553–566. https://doi.org/10.1002/bmc.835

Metrol. Meas. Syst., Vol. 28 (2021), No. 4, pp. 803–812
DOI: 10.24425/mms.2021.138578

[4] Schubert, J. K., Spittler, K. H., Braun, G., Geiger, K., & Guttmann, J. (2001). CO_2-controlled sampling of alveolar gas in mechanically ventilated patients. *Journal of Applied Physiology*, *90*(2), 486–492. https://doi.org/10.1152/jappl.2001.90.2.486

[5] Levitzky, M. G. (2013). *Pulmonary Physiology* (8th ed.). McGraw-Hill Education.

[6] Singh, O. P., & Malarvili, M. B. (2018). Review of infrared carbon-dioxide sensors and capnogram features for developing asthma-monitoring device. *Journal of Clinical and Diagnostic Research*, *12*(10). https://doi.org/10.7860/JCDR/2018/35870.12099

[7] Singh, O. P., Howe, T. A., & Malarvili, M. B. (2018). Real-time human respiration carbon dioxide measurement device for cardiorespiratory assessment. *Journal of Breath Research*, *12*(2), 026003. https://doi.org/10.1088/1752-7163/aa8dbd

[8] Chen, H.-Y., & Chen, C. (2019). Development of a Breath Analyzer for O_2 and CO_2 Measurement. *The Open Biomedical Engineering Journal*, *13*(1), 21–32. https://doi.org/10.2174/1874120701913010021

[9] Mikołajczyk, J., Bielecki, Z., Stacewicz, T., Smulko, J., Wojtas, J., Szabra, D., Lentka, Ł., Prokopiuk, A., & Magryta, P. (2016). Detection of gaseous compounds with different techniques. *Metrology and Measurement Systems*, *23*(2). https://doi.org/10.1515/mms-2016-0026

[10] Prokopiuk, A. (2017). Optoelectronics sensors of hydrocarbons based on NDIR technique. *Proceedings of SPIE – The International Society for Optical Engineering*, 10455. https://doi.org/10.1117/12.2282779

[11] Hamamatsu. (2021, September 2). *Mid infrared LED L13201-0430M*. http://www.hamamatsu.com.cn/UserFiles/upload/file/20190527/l13201_series_kled1069e.pdf

[12] Pike Technologies. (2021). *Stainless Steel Short-Path Gas Cells*. https://www.piketech.com/product/stainless-steel-short-path-gas-cells/

[13] Elliot Scientific. (2021, September 2). *BPF 4260-120 Iridian mid-IR Filter*. https://elliotscientific.com/Iridian-BPF-4260-120

[14] Vigo. (2021, September 2). *PV-3TE-5*. https://vigo.com.pl/produkty/pv-3te/

[15] Richards, P. L. (1994). Bolometers for infrared and millimeter waves. *Journal of Applied Physics*, *76*(1), 1–24. https://doi.org/10.1063/1.357128

[16] American Thoracic Society. (2005). ATS / ERS Recommendations for Standardized Procedures for the Online and Offline Measurement of Exhaled Lower Respiratory Nitric Oxide and Nasal Nitric Oxide, 2005. *American Journal of Respiratory and Critical Care Medicine*, *171*(8), 912–930. https://doi.org/10.1164/rccm.200406-710ST

[17] Mansour, E., Vishinkin, R., Rihet, S., Saliba, W., Fish, F., Sarfati, P., & Haick, H. (2020). Measurement of temperature and relative humidity in exhaled breath. *Sensors and Actuators B: Chemical*, *304*, 127371. https://doi.org/10.1016/j.snb.2019.127371

[18] UTECH Co., Ltd. (2021, September 2). *UT100C Handheld Capnograph Vital Signs Monitor*. https://www.chinautech.com/ut100c-capnograph-monitor-and-pulse-oximeter-etco2-spo2-pulse-rate-.html

[19] Memmert. (2021, September 2). *Universal oven UF30*. https://www.memmert.com/products/heating-drying-ovens/universal-oven/UF30/

Zbigniew Bielecki received the PhD degree from Military University of Technology (MUT), Warsaw, Poland, in 1992. He is currently Full Professor with the Institute of Optoelectronics MUT. He has authored or coauthored 4 books, 19 book chapters, over 60 journal articles (JCR) and over 200 conference publications. His research activity is focused on detection of optical signals.

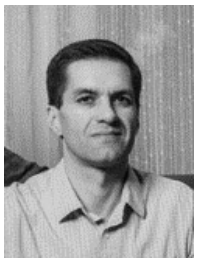

Jacek Wojtas received his PhD degree in Electronics in 2007. He is a member of the IEEE Photonic Society, the Optical Society and the Committee of Metrology and Scientific Equipment of the Polish Academy of Sciences as well as member of the Metrology Council appointed by the Polish Minister of Development. Professor of MUT, expert in optical signal detection and optoelectronic metrology. His research is focused on the use of state-of-the-art optoelectronic technology in gas sensors. He has more than 230 scientific publications and is an associate or guest editor in 3 JCR journals, and reviewer in over 20 journals and grant agencies.

Artur Prokopiuk obtained the MSc degree in Optoelectronics and Ph.D. in Automation, Electronics and Electrical Engineering from the Military University of Technology (MUT), Warsaw, Poland, in 1997 and 2021, respectively. He is currently Research Assistant with the MUT, Poland.